FIT-GNN: Faster Inference Time for GNNs that 'FIT' in Memory Using Coarsening

Shubhajit Roy[*]   *royshubhajit@iitgn.ac.in*
Indian Institute of Technology Gandhinagar

Hrriday Ruparel[*]   *hrriday.ruparel@iitgn.ac.in*
Indian Institute of Technology Gandhinagar

Kishan Ved   *kishan.ved@iitgn.ac.in*
Indian Institute of Technology Gandhinagar

Anirban Dasgupta   *anirbandg@iitgn.ac.in*
Indian Institute of Technology Gandhinagar

Abstract

Scalability of Graph Neural Networks (GNNs) remains a significant challenge. To tackle this, methods like coarsening, condensation, and computation trees are used to train on a smaller graph, resulting in faster computation. Nonetheless, prior research has not adequately addressed the computational costs during the inference phase. This paper presents a novel approach to improve the scalability of GNNs by reducing computational burden during the inference phase using graph coarsening. We demonstrate two different methods – Extra Nodes and Cluster Nodes. Our study extends the application of graph coarsening for graph-level tasks, including graph classification and graph regression. We conduct extensive experiments on multiple benchmark datasets to evaluate the performance of our approach. Our results show that the proposed method achieves orders of magnitude improvements in single-node inference time compared to traditional approaches. Furthermore, it significantly reduces memory consumption for node and graph classification and regression tasks, enabling efficient training and inference on low-resource devices where conventional methods are impractical. Notably, these computational advantages are achieved while maintaining competitive performance relative to baseline models.

1 Introduction

Graph Neural Networks (GNNs) have demonstrated remarkable versatility and modeling capabilities. However, several challenges still hinder their widespread applicability, with scalability being the most significant concern. This scalability issue affects both the training and inference phases. Previous research has sought to mitigate the high training computation cost by using three broad categories of methods: 1. Training every iteration on a sampled subgraph 2. Training on a coarsened graph generated from a coarsening algorithm 3. Training on a synthetic graph that mimics the original graph. Unfortunately, these smaller graphs can only be utilized for training purposes and have not alleviated the computational burden during inference since the method mentioned above requires the whole graph during the inference phase. Consequently, for larger graphs, not only do inference times increase, but memory consumption may also exceed limitations.

To mitigate the high computational cost associated with the inference phase, we decompose the original graph G into a collection of subgraphs $\mathcal{G}_s = \{G_1, G_2, \ldots, G_k\}$. This transformation yields substantial

---

[*]Equal contribution

improvements in inference efficiency, achieving up to a **100×** speedup for single-node prediction. Moreover, it significantly reduces memory consumption by as much as **100×** —thereby enabling scalable inference on large-scale graphs comprising millions of edges. We provide a theoretical characterization of the upper bound on the expected size of subgraphs under which our method's time and space complexity remain superior to that of the baselines. Notably, we observe that conventional methods often fail to perform inference on large graphs due to memory constraints, whereas our approach remains effective and scalable in such scenarios.

While partitioning the graphs into subgraphs seems to be a naive transformation, it comes with the cost of information loss corresponding to the edges removed. We overcome this loss by appending additional nodes in the subgraphs using two different methods – **Extra Nodes** and **Cluster Nodes** that respectively append neighboring nodes or representational nodes corresponding to neighboring clusters. These additional nodes resulted in equivalent or better performance in terms of accuracy and error compared to baselines. Our contributions are summarized as follows:

1. We reduce inference time and memory by applying graph coarsening to partition graphs into subgraphs, mitigating information loss through **Extra Node** and **Cluster Node** strategies.

2. We provide a theoretical analysis of our approach, establishing a lower inference computational complexity compared to baselines.

3. Our method scales well to extremely large graphs that baselines fail to process, while consistently delivering strong performance on 13 real-world datasets.
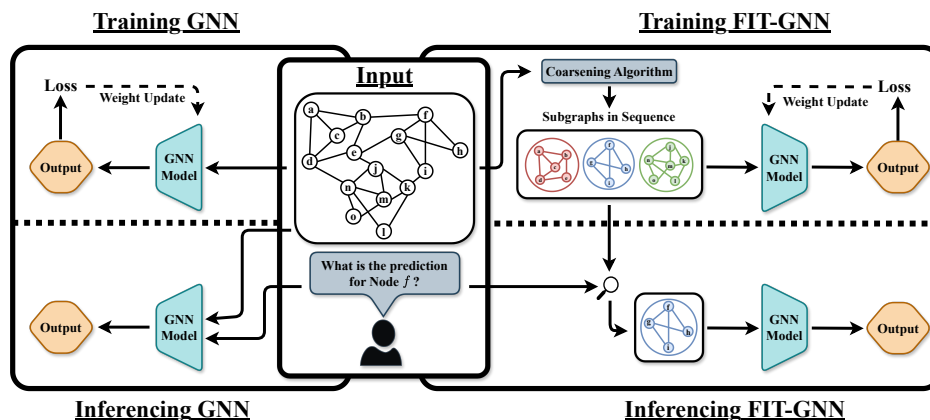

Figure 1: The Figure shows the overall pipeline of our proposed method and its comparison with traditional training and inference of GNNs. This pipeline is made for node-level tasks.

2   Related Work

The aim of reducing computational costs has been approached through various methods. Research by Chiang et al. (2019) and Zeng et al. (2020) uses a subgraph sampling technique, where a small subgraph is sampled at each training iteration for GNN training. Other methods, including layer-wise sampling and mini-batch training, have been explored by Chen et al. (2018a;b); Cong et al. (2020); Zou et al. (2019). Additionally, Fahrbach et al. (2020) introduced a coarsening algorithm based on Schur complements to create node embeddings in large graphs, while Huang et al. (2021) [**SGGC**] applied GNNs to coarsened graphs, reducing nodes and edges to lower training time. Kumar et al. (2023); Joly & Keriven (2024); Kataria et al. (2024); Dickens et al. (2024) also proposed different coarsening algorithms for scalable training approaches. Jin et al. (2021) [**GCOND**], Wang et al. (2024) [**GC-SNTK**] presented algorithms to generate a synthetic graph that mimics the original graph. However, their approach generates model-specific synthetic graphs that require training on the whole dataset, which defeats the purpose of reducing computational burden. Gupta et al. (2025) [**BONSAI**] addressed this issue by looking into computational trees and training on just the relevant computational trees. However, these approaches do not decrease inference time since the inference phase takes the whole graph as input. Xue et al. (2023) shifted the training process to subgraph-level, using coarsening algorithms to split the graph into k-subgraphs and recommending a multi-device

training approach. In the graph-level task, Jin et al. (2022) [**DOSCOND**] and Xu et al. (2023) [**KIDD**] tackled the graph classification problem following up on the approach of GCOND and GC-SNTK. However, the graph regression problem was not explored in this direction.

3 Preliminaries

Graph Notations: Given an undirected graph $G = (V, E, X, W)$, V is the vertex set, E is the edge set, $X \in \mathbb{R}^{n \times d}$ is the feature matrix, and W is the edge weight matrix. Let $|V| = n$ be the number of nodes and $|E| = m$ be the number of edges. Let $A \in \mathbb{R}^{n \times n}$ be the adjacency matrix of G where A_{ij} is the edge weight between nodes v_i and v_j, and d_i is the degree of the node v_i. $D \in \mathbb{R}^{n \times n}$ is a diagonal degree matrix with ith diagonal element as d_i. We denote $\mathcal{N}_j(v_i)$ as the j-hop neighbourhood of node $v_i \in V$. **Graph Neural Network:** Graph Neural Network is a neural network designed to work for graph-structured data. The representation of each node in the graph is updated recursively by aggregation and transforming the node representations of its neighbors. Kipf & Welling (2017) introduced Graph Convolutional Network (GCN) as follows:

$$X^{(l+1)} = \sigma(\tilde{D}^{-\frac{1}{2}} \tilde{A} \tilde{D}^{-\frac{1}{2}} X^{(l)} \mathcal{W}^{(l)}) \tag{1}$$

where $X^{(l)}$ is the node representation after l layers, $\tilde{A} = A + I$, $\tilde{D} = D + I$, I is the identity matrix of same dimension as A. $\mathcal{W}^{(l)}$ is the learnable parameter and σ is a non-linear activation function.

Graph Coarsening and Graph Partitioning: Loukas (2019) discussed multiple coarsening algorithms which create a coarsened graph $G' = (V', E', X', W')$ from a given graph $G = (V, E, X, W)$. We refer the vertex set $V' = \{v'_1, v'_2, \ldots, v'_k\}$ of G' as *coarsened nodes*. Given a coarsening ratio $r \in [0, 1]$, we have $k = \lfloor n \times r \rfloor$, $k \in \mathbb{Z}$. We can interpret it as creating k disjoint partitions, $C_1, C_2, \ldots, C_k$, from a graph of n nodes. Mathematically, we create a partition matrix $P \in \{0, 1\}^{n \times k}$, where $P_{ij} = 1$ if and only if node $v_i \in C_j$. $X' = P^\top X$ is the coarsened node representation. $A' = P^\top A P$ is the adjacency matrix of G'. Similarly, the corresponding degree matrix $D' = P^\top D P$. SGGC (Huang et al., 2021) used normalized partition matrix $\mathcal{P} = P C^{-\frac{1}{2}}$, where C is defined as a diagonal matrix with diagonal entries $C_{jj} = |C_j|, j = 1, 2, \ldots, k$.

Along with G', we create a set of disjoint subgraphs $\mathcal{G}_s = \{G_1, G_2, \ldots, G_k\}$ corresponding to the partitions $C_1, C_2, \ldots, C_k$. The number of nodes in each partition C_i is denoted by n_i. Each subgraph G_i is the induced subgraph of G formed by the nodes in C_i. A_i and D_i are the adjacency and degree matrix of G_i respectively.
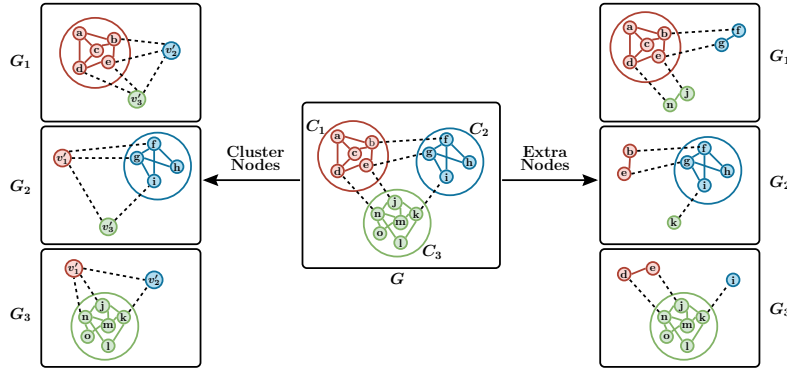
Figure 2: Figure showing the comparison between the Extra Node Method and the Cluster Node Method of appending additional nodes in G_1, G_2, G_3.

4 Methodology

In SGGC, a graph G is reduced to G' using a partition matrix P generated from the coarsening algorithm. The labels for the coarsened graph are $Y' = \arg\max(P^\top Y)$, where Y is the label matrix of G storing the one-hot encoding of the label of each node for the node classification task. Training is carried out on

the coarsened graph G' using Y' as the label information. While this approach is novel, essential label information is lost. For instance, suppose a node $v' \in G'$ is a combination of $v_i, v_j, v_k \in G$ where v_i, v_j, v_k are test nodes. Let us assume that the classes of v_i, v_j, v_k are $0, 0, 2$ respectively. $\arg\max$ will take the majority label and assign class 0 to v'. Hence, the model will be trained to predict only the class 0, leading to the discarding of the quantification of the model's performance on predicting less represented nodes.

Similarly, to explore another node-level task, such as node regression, aggregation functions such as the mean of regression targets wouldn't be appropriate because they lose the variance of the targets. To mitigate label information loss, we use original label information without any aggregation function like $\arg\max$ or mean, thus motivating us to follow a subgraph-level training process.

However, partitioning the graph into subgraphs leads to a loss of neighborhood information at the periphery of subgraphs. To tackle this, we append nodes in two ways after partitioning:

- **Extra Nodes:** Adding the 1-hop neighbouring nodes, namely Extra Nodes, in each subgraph G_i denoted by $\mathcal{E}_{G_i}$. Xue et al. (2023) introduced this approach to reduce information loss after partitioning. We add a unit weight edge if two nodes in $\mathcal{E}_{G_i}$ are connected in G. Node embedding of $v \in \mathcal{E}_{G_i}$ is $x_v \in X$.

$$\mathcal{E}_{G_i} = \bigcup_{v \in G_i} \{u \in V : u \in \mathcal{N}_1(v) \wedge u \notin G_i\} \tag{2}$$

- **Cluster Nodes:** Although adding 1-hop neighboring nodes in the subgraph helps recover lost information after partition, for multi-layered GNN models, information loss will persist. Instead of adding the neighboring nodes, we will add Cluster Nodes, which represent the neighboring clusters, denoted by $\mathcal{C}_{G_i}$. Liu et al. (2024) introduced this method to add nodes in the graph instead of adding to separate subgraphs. They also added cross-cluster edges among these Cluster Nodes and proposed a subgraph sampling-based method on the modified graph. In our work, we add cross-cluster edges. For each node $t \in \mathcal{C}_{G_i}$, the node embedding $x_t = X'_t$.

$$\mathcal{C}_{G_i} = \bigcup_{v \in \mathcal{E}_{G_i}} \{t : P_{v,t} \neq 0\} \tag{3}$$

Figure 2 illustrates appending these additional nodes using these approaches. The dashed line shows which nodes are added as part of these additional nodes. For subgraph-level training, specifically for node-level tasks, the newly appended nodes do not contribute to the weight update as the loss is not backpropagated based on the predictions of these nodes. This is done since the appended nodes might contain information from the test nodes. Therefore, a boolean array $mask_i$ is created for each subgraph G_i such that $True$ is set for nodes that actually belong to the subgraph G_i (not as an Extra Node or Cluster Node) and are training nodes; otherwise, $False$.

Lemma 4.1. *Models with 1 layer of GNN cannot distinguish between G and $\mathcal{G}_s$ when **Extra Nodes** method is used. (Proof in Appendix A.1)*

Using the **Cluster Nodes** approach to append additional nodes to subgraphs is better for two reasons:

- From Equation 2 and 3, we can say that $\sum_i |\mathcal{E}_{G_i}| \geq \sum_i |\mathcal{C}_{G_i}|$. This is because, using Extra Nodes, we add all the neighboring nodes. However, using Cluster Nodes, we only add one representative node for each neighboring cluster. Hence, the time taken to train and infer these modified subgraphs with Cluster Nodes is at most that with Extra Nodes.

- Lemma 4.1 shows that the Extra Nodes approach reduces the information loss due to partitioning for 1 Layer of GNN. However, with multiple layers of GNN, longer dependencies are not captured. In contrast, the Cluster Nodes approach overcomes this by computing a single Cluster Node's representation as a combination of features of all the nodes present in the corresponding cluster. This results in sharing further node information in 1-hop. Additionally, the transfer of information from one cluster to another is captured.

Algorithm 1 Training GNN (Train on $\mathcal{G}_s$)

Require: $G = (V, E, X)$; Labels Y; Node-Model M; Loss ℓ; Number of Layers L
1: Apply a coarsening algorithm on G, and output a normalized partition matrix P.
2: Construct $\mathcal{G}_s = \{G_1(V_1, E_1, X_1), G_2(V_2, E_2, X_2), \ldots, G_k(V_k, E_k, X_k)\}$ using P;
3: **if** Append additional nodes **then**
4:      Append $\mathcal{E}_{G_i}$ or $\mathcal{C}_{G_i}$ to each G_i ▷ Based on method of appending nodes
5: **end if**
6: Construct mask for each subgraph $Mask = \{mask_1, mask_2, \ldots, mask_k\}$;
7: Construct label matrix $\{Y_1, Y_2, \ldots, Y_k\}$ for $\mathcal{G}_s$;
8: $O \leftarrow []$; $Y_{\text{Collected}} \leftarrow []$;
9: **for** each subgraph G_i in $\mathcal{G}_s$ **do**
10:      $O_i = M(L, A_i, D_i, X_i)$;   ▷ Algorithm 4
11:      $O.append(O_i[mask_i])$;
12:      $Y_{\text{Collected}}.append(Y_i[mask_i])$;
13: **end for**
14: $Loss = \ell(O, Y_{\text{Collected}})$;
15: Train M to minimize $Loss$;

4.1 Node-level Task

We use Algorithm 4 with L number of layers to create a standard GNN model M for node-level tasks. While we use Algorithm 3 to train a model on the coarsened graph G', we propose Algorithm 1 to train a model on the set of subgraphs $\mathcal{G}_s$. Algorithm 3 utilizes the partition matrix P generated by the coarsening algorithm to construct and train on the coarsened graph G' and the coarsened label information Y'. On the other hand, our proposed Algorithm 1 uses the same partition matrix P to construct and train on subgraphs $\mathcal{G}_s$ using original label information Y. For the node classification task, $\arg\max$ is used for creating Y' for G' and CrossEntropy as a loss function. For the node regression task, we do not create G'. Mean Absolute Error (MAE) is used as the loss function.

4.2 Graph-level Task

For a given graph $G \in \mathcal{D}$, we create G' and $\mathcal{G}_s = \{G_1, G_2, \ldots, G_k\}$. Since G' is a single graph and $\mathcal{G}_s$ is a set of subgraphs, we use Algorithm 5 to create a model that trains on G' and Algorithm 2 to create a model that trains on $\mathcal{G}_s$. We use the CrossEntropy loss function for the graph classification task and the Mean Absolute Error (MAE) for the graph regression task.

Algorithm 2 Graph-Model-$\mathcal{G}_s(\mathcal{G}_s, L)$

Require: $\mathcal{G}_s = \{G_1, G_2, \ldots, G_k\}$; Number of Layers L;
1: $\tilde{X} \leftarrow []$
2: **for** each subgraph $G_i \in \mathcal{G}_s$ **do**
3:      **for** $j = 1$ to L **do**
4:          $X_i^{(j)} = \sigma(\tilde{D}_i^{-\frac{1}{2}} \tilde{A}_i \tilde{D}_i^{-\frac{1}{2}} X_i^{(j-1)} \mathcal{W}^{(j-1)})$ ▷ Equation 1
5:      **end for**
6:      $\tilde{X}.stack(X_i^{(L)})$ ▷ Stack along row axis
7: **end for**
8: $\bar{X} = \text{MaxPooling}(\tilde{X})$
9: $Z = \bar{X}\mathcal{W}^{(L)}$
10: **return** Z

4.3 Time and Space Complexity

In Equation 1, the matrix dimensions are as follows: $\tilde{A}$ has dimensions $(n \times n)$, $X^{(l)}$ is of dimensions $(n \times d)$, and $\mathcal{W}^{(l)}$ has dimensions $(d \times d)$. Time complexity for one layer of GNN computation is $\mathcal{O}(n^2d + nd^2)$. If we take L layers, then the total time is $\mathcal{O}(Ln^2d + Lnd^2)$. The space complexity is $\mathcal{O}(n^2 + Lnd + Ld^2)$. When we compute on a sparse graph, the time complexity is $\mathcal{O}(m + Lnd^2)$ and space complexity is $\mathcal{O}(m + Lnd + Ld^2)$. The complexity is based on GCN. For other architectures like GAT (Veličković et al., 2018), the complexity changes.

Table 1: Training and inference time and space complexity of FIT-GNN compared to classical and SGGC approaches.

(a) Time Complexity			**(b) Space Complexity**		
	Train	**Inference**		**Train**	**Inference**
Classical	$nd^2 + n^2d$	$nd^2 + n^2d$	**Classical**	$n^2 + nd + d^2$	$n^2 + nd + d^2$
SGGC	$kd^2 + k^2d$	$nd^2 + n^2d$	**SGGC**	$k^2 + kd + d^2$	$n^2 + nd + d^2$
FIT-GNN	$kd^2 + k^2d$ $+ \sum_{i=1}^{k}[\bar{n}_i^2 d + \bar{n}_i d^2]$	$\sum_{i=1}^{k}[\bar{n}_i^2 d + \bar{n}_i d^2]$	**FIT-GNN**	$k^2 + kd + d^2$ $+ \max_{i=1}[\bar{n}_i^2 + \bar{n}_i d]$	$d^2 + \max_{i=1}[\bar{n}_i^2 + \bar{n}_i d]$

SGGC improved the time and space complexity (Table 1) for training the network by reducing the number of nodes from n to k. However, the inference time and space complexity remain the same.

Let us compare three different models. One is the classical model, where no coarsening or partitioning is done; the second is SGGC, where training is performed on a smaller graph G' and inference on G; the third is our approach, FIT-GNN, where both training and inference are performed on $\mathcal{G}_s$.

The inference time complexity of our model is $\mathcal{O}\left(\sum_{i=1}^{k}[\bar{n}_i^2 d + \bar{n}_i d^2]\right)$, where $\bar{n}_i = n_i + \phi_i$ and ϕ_i is the number of additional nodes appended in each subgraph. Table 1 compares different approaches.

Lemma 4.2. *The inference time complexity $\mathcal{O}\left(\sum_{i=1}^{k}[(n_i + \phi_i)^2 d + (n_i + \phi_i)d^2]\right)$ is at most $\mathcal{O}\left(n^2 d + nd^2\right)$ if $\mathbb{E}[n_i + \phi_i] \leq \sqrt{\frac{d^2}{4} + \frac{d}{r} + \frac{n}{r} - \mathrm{Var}(n_i + \phi_i)} - \frac{d}{2}$, where $\mathbb{E}[n_i + \phi_i]$ is the expected number of nodes in each modified subgraph and $\mathrm{Var}(n_i + \phi_i)$ is the variance of number nodes in each modified subgraph.*

Proof. We can expand our inference time complexity as follows:

$$\sum_{i=1}^{k}[(n_i + \phi_i)^2 d + (n_i + \phi_i)d^2] = nd^2 + d\left[\sum_{i=1}^{k} n_i^2 + \sum_{i=1}^{k} \phi_i^2 + 2\sum_{i=1}^{k} n_i\phi_i + d\sum_{i=1}^{k} \phi_i\right]$$

Now, define expected number of nodes in each subgraph $\mathbb{E}[n_i] := \frac{1}{k}\sum_{i=1}^{k} n_i = \frac{n}{k} = \frac{1}{r}$ (since $k = nr$) and expected number of additional nodes appended in each subgraph $\mathbb{E}[\phi_i] := \frac{1}{k}\sum_{i=1}^{k} \phi_i$. We also define the variances and covariance,

$$\mathrm{Var}(n_i) := \frac{1}{k}\sum_{i=1}^{k} n_i^2 - \mathbb{E}[n_i]^2, \quad \mathrm{Var}(\phi_i) := \frac{1}{k}\sum_{i=1}^{k} \phi_i^2 - \mathbb{E}[\phi_i]^2, \quad \mathrm{Cov}(n_i, \phi_i) = \mathrm{Cov} := \frac{1}{k}\sum_{i=1}^{k} \phi_i n_i - \mathbb{E}[\phi_i]\mathbb{E}[n_i]$$

We can also write,

$$\mathrm{Var}(n_i + \phi_i) = \frac{1}{k}\sum_{i=1}^{k}(n_i + \phi_i)^2 - (\mathbb{E}[n_i] + \mathbb{E}[\phi_i])^2 = \mathrm{Var}(n_i) + \mathrm{Var}(\phi_i) + 2\mathrm{Cov}(n_i, \phi_i)$$

Using the definitions above, we can say:

$$\sum_{i=1}^{k}[(n_i + \phi_i)^2 d + (n_i + \phi_i)d^2] = nd^2 + d\left[\sum_{i=1}^{k} n_i^2 + \sum_{i=1}^{k} \phi_i^2 + 2\sum_{i=1}^{k} n_i\phi_i + d\sum_{i=1}^{k} \phi_i\right]$$

$$= nd^2 + d\left[k(\mathrm{Var}(n_i) + \mathbb{E}[n_i]^2) + k(\mathrm{Var}(\phi_i) + \mathbb{E}[\phi_i]^2) + 2k(\mathrm{Cov}(n_i, \phi_i) + \mathbb{E}[n_i]\mathbb{E}[\phi_i]) + dk\mathbb{E}[\phi_i]\right]$$

$$= nd^2 + nd\left[r\mathrm{Var}(n_i) + \frac{1}{r} + r\mathrm{Var}(\phi_i) + r\mathbb{E}[\phi_i]^2 + 2r\mathrm{Cov}(n_i, \phi_i) + 2\mathbb{E}[\phi_i] + rd\mathbb{E}[\phi_i]\right]$$

$$= nd^2 + nd\left[r\mathbb{E}[\phi_i]^2 + (2 + rd)\mathbb{E}[\phi_i] + r\mathrm{Var}(n_i + \phi_i) + \frac{1}{r}\right]$$

Given, $\mathbb{E}[n_i + \phi_i] \le \sqrt{\frac{d^2}{4} + \frac{d}{r} + \frac{n}{r} - \mathrm{Var}(n_i + \phi_i)} - \frac{d}{2} \Rightarrow \mathbb{E}[\phi_i] \le \sqrt{\frac{d^2}{4} + \frac{d}{r} + \frac{n}{r} - \mathrm{Var}(n_i + \phi_i)} - (\frac{d}{2} + \frac{1}{r})$. Using this, we can say the following:

$$\sum_{i=1}^{k} [(n_i + \phi_i)^2 d + (n_i + \phi_i) d^2] = nd^2 + nd \left[r\mathbb{E}[\phi_i]^2 + (2 + rd)\mathbb{E}[\phi_i] + r\mathrm{Var}(n_i + \phi_i) + \frac{1}{r} \right]$$

$$\le nd^2 + nd \left[r\left(\frac{d^2}{4} + \frac{d}{r} + \frac{n}{r} - \mathrm{Var}(n_i + \phi_i) + \frac{d^2}{4} + \frac{1}{r^2} + \frac{d}{r} - 2\left(\frac{d}{2} + \frac{1}{r} \right) \sqrt{\Delta} \right) \right.$$

$$\left. + 2\sqrt{\Delta} - 2\left(\frac{d}{2} + \frac{1}{r} \right) + rd\sqrt{\Delta} - rd\left(\frac{d}{2} + \frac{1}{r} \right) + r\mathrm{Var}(n_i + \phi_i) + \frac{1}{r} \right]$$

$$\left(\text{where } \frac{d^2}{4} + \frac{d}{r} + \frac{n}{r} - \mathrm{Var}(n_i + \phi_i) = \Delta \right)$$

$$= nd^2 + n^2 d$$

Hence, $\sum_{i=1}^{k} [(n_i + \phi_i)^2 d + (n_i + \phi_i) d^2] \le n^2 d + nd^2$. □

Corollary 4.3. $\mathbb{E}[\phi_i]$ *has a positive upper bound when* $\mathrm{Var}(n_i + \phi_i) \le \frac{n}{r} - \frac{1}{r^2}$.

Proof. From Lemma 4.2, we know the upper bound of $\mathbb{E}[\phi_i]$ is $\sqrt{\frac{d^2}{4} + \frac{d}{r} + \frac{n}{r} - \mathrm{Var}(n_i + \phi_i)} - \left(\frac{d}{2} + \frac{1}{r} \right)$.

If $\sqrt{\frac{d^2}{4} + \frac{d}{r} + \frac{n}{r} - \mathrm{Var}(n_i + \phi_i)} - \left(\frac{d}{2} + \frac{1}{r} \right) \ge 0$, then we can say the following:

$$\sqrt{\frac{d^2}{4} + \frac{d}{r} + \frac{n}{r} - \mathrm{Var}(n_i + \phi_i)} - \left(\frac{d}{2} + \frac{1}{r} \right) \ge 0 \Rightarrow \frac{d^2}{4} + \frac{d}{r} + \frac{n}{r} - \mathrm{Var}(n_i + \phi_i) \ge \left(\frac{d}{2} + \frac{1}{r} \right)^2$$

$$\Rightarrow \mathrm{Var}(n_i + \phi_i) \le \frac{n}{r} - \frac{1}{r^2}$$

□

For a given graph, when the above conditions are satisfied, our approach has better inference time and space complexity than other approaches. From Corollary 4.3, we can understand that it is ideal to have similarly sized subgraphs. For more details on time and space complexity, refer to Section C in the Appendix.

5 Experiments

Let training on the coarsened graph G' be referred to as **Gc-train**, subgraph-level training as **Gs-train**, and subgraph-level inference process as **Gs-infer**. Once we have constructed G' and $\mathcal{G}_s$, we train FIT-GNN in 4 different setups:

- **Gc-train-to-Gs-train**: Train the GNN model on G' as per Algorithm 3, then use the learned weight as an initialization for subgraph-level training and final inference on $\mathcal{G}_s$. We examine whether pretraining on G' (which requires less time) followed by fine-tuning on $\mathcal{G}_s$ for fewer epochs can improve performance.

- **Gc-train-to-Gs-infer**: Train the GNN model on G' as per Algorithm 3, then infer on $\mathcal{G}_s$ using the learned weights. We explore whether training solely on the G' is sufficient for inference on $\mathcal{G}_s$. This setting presents a computationally efficient option, allowing users with limited resources to obtain results close to the best reported.

- **Gs-train-to-Gs-infer**: Perform subgraph-level training and inference on $\mathcal{G}_s$.

- **Gc-train-to-Gc-infer**: Unlike node-level tasks, for graph-level tasks, inference can be done directly on G' because the label corresponds to the entire graph and not to individual nodes. Therefore, even with a reduced graph representation, meaningful inference is possible. Therefore, in this setup for graph-level tasks only, we train and infer on G'.

All four setups can be applied to graph-level tasks. For the node classification task, we apply all setups except **Gc-train-to-Gc-infer**. For the node regression task, we only perform **Gs-train-to-Gs-infer** because a coarsened graph is not created for node regression datasets.

Dataset descriptions and details related to hyperparameters, device configuration, and key packages used for the experiments are in Section D and E. Source code: https://github.com/Roy-Shubhajit/FIT-GNN.

Table 2: Datasets and corresponding splits used in our experiments. 'c' denotes the number of classes in node classification datasets. Public split "fixed" by Yang et al. (2016) is used for *Cora*, *Citeseer*, and *PubMed*. For the "random" split, we use 20 nodes per class for training, 30 per class for validation, and the rest for testing. For *QM9*, we follow Gilmer et al. (2017) and predict one property from each broad category: dipole moment (μ), HOMO-LUMO gap ($\epsilon_{\mathrm{HOMO}} - \epsilon_{\mathrm{LUMO}}$), zero-point vibration energy (ZPVE), and atomization energy (U^{ATOM}) at 298.15K.

Task	Dataset (Reference)	Train	Val	Test
Node Regression	*Chameleon* (Rozemberczki et al., 2021)	30%	20%	50%
	Crocodile (Rozemberczki et al., 2021)	30%	20%	50%
	Squirrel (Rozemberczki et al., 2021)	30%	20%	50%
Node Classification	*Cora* (McCallum et al., 2000)	$20 \times c$	$30 \times c$	Rest
	Citeseer (Giles et al., 1998)	$20 \times c$	$30 \times c$	Rest
	Pubmed (Sen et al., 2008)	$20 \times c$	$30 \times c$	Rest
	Coauthor Physics (Shchur et al., 2018)	$20 \times c$	$30 \times c$	Rest
	DBLP (Tang et al., 2008)	$20 \times c$	$30 \times c$	Rest
	OGBN-Products (Hu et al., 2020)	$20 \times c$	$30 \times c$	Rest
Graph Regression	*QM9* (Wu et al., 2018)	50%	25%	25%
	ZINC (Subset) (Gómez-Bombarelli et al., 2018)	50%	25%	25%
Graph Classification	*PROTEINS* (Morris et al., 2020)	50%	25%	25%
	AIDS (Morris et al., 2020)	50%	25%	25%

6 Result and Analysis

6.1 Model Performance

Node Classification: Table 4 shows the results for node classification accuracy (mean and standard deviation of the top 10 accuracies) with coarsening ratios 0.3 and 0.5 using the **Cluster Nodes** approach. Comparison with other coarsening ratios is in Table 12. Results show that the accuracy is comparable to the baselines. Figure 3 shows the comparison of performance between different experimental setups for different methods of appending nodes on the *Cora* dataset. From the Figure, we observe that **Gc-train-to-Gs-train** offers the best result among the three experimental setups for the node classification task. For the 'None' method of appending nodes, where no additional nodes are added to each subgraph, we notice that it performs poorly compared to other methods, indicating that

Table 3: Results on OGBN-Products. FIT-GNN model uses a coarsening ratio 0.5. **variation_neighborhoods** coarsening algorithm is used. OOM means Out Of Memory.

Full (Luo et al., 2024)	0.823 ± 0.001
SGGC	OOM
GCOND	OOM
BONSAI	OOM
FIT-GNN	$\mathbf{0.894 \pm 0.000}$

the Extra Node and Cluster Node methods indeed provide additional information for better empirical performance. We also observe in the 'None' method that, with an increase in the coarsening ratio, the performance drops. This is because, as the coarsening ratio increases, the size of each subgraph gets smaller, hence more edges are cut due to partitioning, leading to more information loss. For the **Gc-train-to-Gs-infer** method, we observe that the performance drops as the coarsening ratio increases. This can be argued because of the change in the distribution of the coarsened graph and the set of subgraphs. When training on G_s, the distribution in the train and test sets is similar, hence attaining better performance. While comparing the methods of appending nodes, we infer that the Cluster Node method is performing similarly compared to

Table 4: Results for node classification tasks with accuracy as the metric (higher is better). We use the Cluster Nodes method to append additional nodes to subgraphs and **Gs-train-to-Gs-infer** as experimental setup. **variation_neighborhoods** coarsening algorithm is used.

Methods	Models	Reduction Ratio (r)	Dataset				
			Cora	*Citeseer*	*Pubmed*	*DBLP*	*Physics*
Full	GCN	1.0	0.821 ± 0.002	0.706 ± 0.002	0.768 ± 0.020	0.724 ± 0.002	$\mathbf{0.933 \pm 0.000}$
	GAT	1.0	0.809 ± 0.004	0.700 ± 0.003	0.740 ± 0.004	0.713 ± 0.004	0.909 ± 0.008
SGGC	GCN	0.3	0.808 ± 0.003	0.700 ± 0.001	0.773 ± 0.002	0.737 ± 0.011	0.928 ± 0.003
		0.5	0.808 ± 0.001	0.716 ± 0.002	$\colorbox{green}{0.793 \pm 0.002}$	0.733 ± 0.008	0.931 ± 0.004
	GAT	0.3	0.686 ± 0.010	0.635 ± 0.021	0.773 ± 0.002	0.626 ± 0.028	0.870 ± 0.016
		0.5	0.641 ± 0.026	0.635 ± 0.024	0.683 ± 0.024	0.604 ± 0.047	0.842 ± 0.018
GCOND	GCN	0.3	0.806 ± 0.003	0.722 ± 0.001	0.779 ± 0.002	0.748 ± 0.001	0.876 ± 0.011
		0.5	0.808 ± 0.004	$\colorbox{green}{\mathbf{0.730 \pm 0.007}}$	0.773 ± 0.004	0.755 ± 0.002	0.804 ± 0.005
	GAT	0.3	0.549 ± 0.080	0.628 ± 0.095	0.370 ± 0.079	0.481 ± 0.034	OOM
		0.5	0.712 ± 0.059	0.501 ± 0.085	0.409 ± 0.044	0.464 ± 0.030	OOM
BONSAI	GCN	0.3	0.722 ± 0.011	0.585 ± 0.003	0.538 ± 0.103	0.683 ± 0.039	0.798 ± 0.007
		0.5	0.701 ± 0.012	0.666 ± 0.001	0.670 ± 0.084	0.702 ± 0.049	0.832 ± 0.016
	GAT	0.3	0.680 ± 0.014	0.566 ± 0.003	0.540 ± 0.096	0.665 ± 0.027	0.791 ± 0.010
		0.5	0.683 ± 0.006	0.579 ± 0.004	0.523 ± 0.133	0.681 ± 0.025	0.812 ± 0.016
FIT-GNN	GCN	0.3	0.800 ± 0.003	0.679 ± 0.003	0.754 ± 0.001	$\colorbox{green}{\mathbf{0.786 \pm 0.001}}$	$\colorbox{green}{0.932 \pm 0.000}$
		0.5	$\colorbox{green}{\mathbf{0.829 \pm 0.002}}$	0.668 ± 0.003	0.761 ± 0.004	0.700 ± 0.001	0.926 ± 0.000
	GAT	0.3	0.761 ± 0.004	0.655 ± 0.005	0.754 ± 0.002	0.771 ± 0.002	0.885 ± 0.004
		0.5	0.792 ± 0.003	0.669 ± 0.004	0.760 ± 0.003	0.720 ± 0.002	0.885 ± 0.003
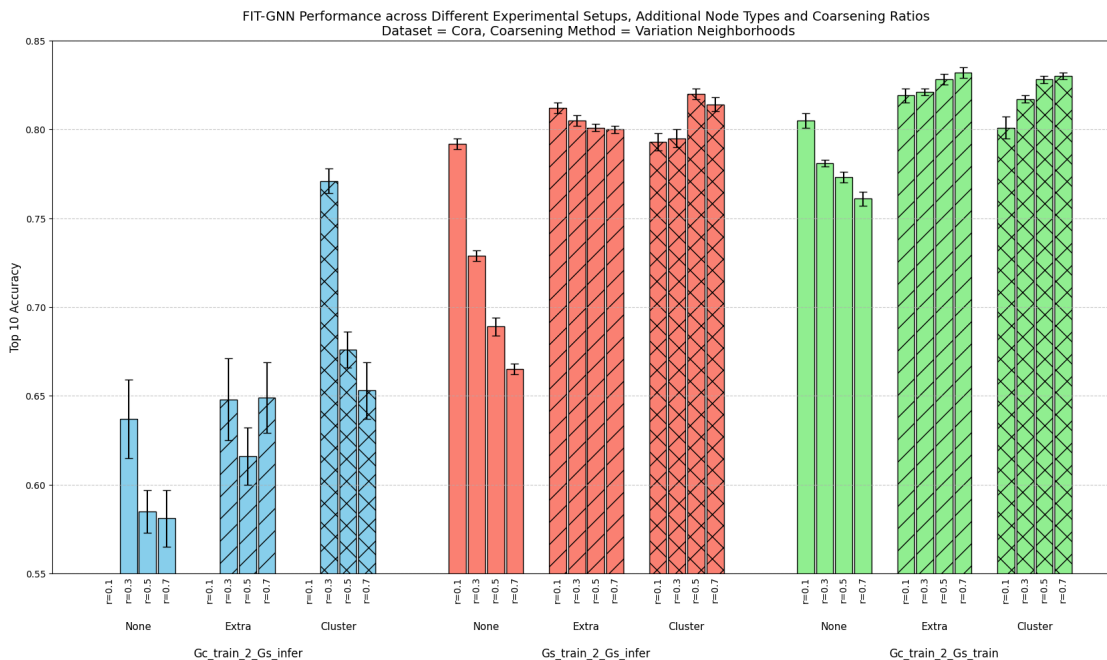
Figure 3: The plot shows the ablation study conducted on the *Cora* dataset to determine which experimental setup performs better than the others. The plot also compares different methods of appending nodes to the subgraphs and how performance changes with varying coarsening ratios. **variation_neighborhoods** coarsening algorithm is used.

the Extra Nodes method, if not better. Table 3 shows results on the *OGBN-Products* dataset. We use the result by Luo et al. (2024) for the full graph setting, which used the OGBN's standard split, while the split used in our work is detailed in Table 2.

Table 5: This table shows the normalized MAE loss (lower is better) for node regression task on different datasets with **Gs-train-to-Gs-infer** experiment setup and **Cluster Nodes** method. **variation_neighborhoods** coarsening algorithm is used.

Methods	Models	Reduction Ratio (r)	Dataset		
			Chameleon	*Crocodile*	*Squirrel*
Full	GCN	1.0	0.852 ± 0.001	0.854 ± 0.000	0.802 ± 0.000
	GAT	1.0	0.846 ± 0.002	0.850 ± 0.000	0.805 ± 0.001
	SAGE	1.0	0.848 ± 0.002	0.850 ± 0.000	0.804 ± 0.000
	GIN	1.0	0.843 ± 0.000	0.852 ± 0.000	0.796 ± 0.000
FIT-GNN	GCN	0.1	0.496 ± 0.005	0.364 ± 0.001	0.663 ± 0.003
		0.3	0.531 ± 0.006	0.369 ± 0.002	0.682 ± 0.002
		0.5	0.531 ± 0.004	0.371 ± 0.001	0.722 ± 0.002
		0.7	0.536 ± 0.009	0.368 ± 0.003	0.696 ± 0.002
	GAT	0.1	0.582 ± 0.029	0.395 ± 0.022	0.734 ± 0.019
		0.3	0.537 ± 0.021	0.383 ± 0.020	0.724 ± 0.020
		0.5	0.556 ± 0.018	0.386 ± 0.018	0.728 ± 0.023
		0.7	0.576 ± 0.018	0.395 ± 0.012	0.746 ± 0.020
	SAGE	0.1	0.506 ± 0.006	$\mathbf{0.309 \pm 0.014}$	$\mathbf{0.589 \pm 0.003}$
		0.3	0.489 ± 0.003	0.315 ± 0.001	0.602 ± 0.003
		0.5	$\mathbf{0.484 \pm 0.004}$	0.317 ± 0.001	0.618 ± 0.002
		0.7	0.539 ± 0.009	0.323 ± 0.000	0.621 ± 0.004
	GIN	0.1	0.769 ± 0.101	0.722 ± 0.098	0.795 ± 0.018
		0.3	0.808 ± 0.056	0.697 ± 0.122	0.796 ± 0.004
		0.5	0.810 ± 0.062	0.730 ± 0.091	0.786 ± 0.032
		0.7	0.792 ± 0.089	0.779 ± 0.102	0.791 ± 0.009

Node Regression: Table 5 presents the node regression error (mean and standard deviation of the lowest 10 MAE). Interestingly, our results demonstrate that utilizing localized subgraphs for inference (FIT-GNN) significantly improves performance compared to full-graph inference. To investigate this counterintuitive performance leap, we conducted a rigorous ablation study (Appendix G). Our analysis indicates that this improvement is driven by the structural properties of the input data during inference rather than the training regime itself. First, partitioning the graph creates localized contexts that are statistically more homogeneous; we observed that the label standard deviation within individual subgraphs is drastically lower than the global variation, presenting a simpler optimization landscape for the model. Second, while coarsening (e.g., at a ratio of $r = 0.5$) causes a vast majority of nodes to lose a significant portion of their distant 2nd-hop neighborhood, this structural loss actually acts as *implicit adversarial pruning*. In these specific heterophilic graphs, long-range information often introduces noise or adversarial signals. By filtering out this noise through coarsening, the model is able to fully exploit the low-variance local structures, ultimately leading to the observed reduction in regression error.

Graph Regression: Table 6 shows the results for the graph regression task on *ZINC (Subset)* and *QM9* dataset. All the results show that the FIT-GNN model's performance is better than the baselines. It is also observed that a lower coarsening ratio yields better loss, which implies that the model performs better on molecular graphs when the subgraph size is large. We observe that finer subgraphs lose out on global information about the molecule, which is necessary for the prediction. Similarly, the performance degrades in the **Gc-train-to-Gc-infer** setup, where we infer on the coarsened graphs. This is because, when a graph is reduced to a smaller graph, the individual node information is lost, which is crucial since, in graphs representing different molecules, components formed by different atoms result in different properties of the molecule.

Graph Classification: Table 7 shows graph classification results on *AIDS* and *PROTEINS* datasets, where training and inference are done on G'. For baselines like DOSCOND and KIDD, we use 'Graph per class', whereas we use 'Reduction Ratio (r)' as a metric to denote how these algorithms reduce the size of training data. DOSCOND and KIDD propose to generate synthetic graphs that mimic the training data distribution.

Table 6: Results on Graph Regression with MAE as metric (lower is better); We use Extra node and **Gs-train-to-Gs-infer** as experimental setup. **variation_neighborhoods** coarsening algorithm is used.

Methods	Models	Reduction Ratio (r)	Dataset				
			ZINC (Subset)	*QM9 (μ)*	*QM9 ($\Delta\epsilon$)*	*QM9 (ZPVE)*	*QM9 (U^{ATOM})*
Full	GCN	1.0	0.743	0.855	1.012	1.102	1.073
	GAT	1.0	0.736	0.919	1.015	1.104	1.066
	SAGE	1.0	0.685	0.885	1.015	1.109	1.076
	GIN	1.0	0.748	0.925	1.053	1.126	1.078
FIT-GNN	GCN	0.1	0.625	0.713	1.223	**0.447**	1.223
		0.3	**0.573**	0.708	0.975	0.473	1.220
		0.5	0.645	0.702	1.153	0.485	1.179
		0.7	0.651	0.715	1.189	0.456	1.240
	GAT	0.1	0.574	0.705	0.940	0.464	0.524
		0.3	0.652	0.708	1.056	0.528	0.564
		0.5	0.620	0.693	1.227	0.475	0.561
		0.7	0.658	**0.686**	1.030	0.491	0.703
	SAGE	0.1	0.735	0.726	**0.739**	0.526	0.905
		0.3	0.671	0.748	0.711	0.602	**0.518**
		0.5	0.695	0.739	0.747	0.606	0.833
		0.7	0.645	0.722	0.677	0.659	1.005
	GIN	0.1	0.644	0.726	0.746	0.494	0.856
		0.3	0.669	0.723	0.761	0.509	0.854
		0.5	0.631	0.725	0.848	0.737	1.058

Therefore, to cover all the graphs in the dataset appropriately, this approach generates {1, 10, 50} graphs per class. However, the graph size is kept similar to the graph size in the training set. These approaches also don't cover the test set. Compared to these baselines, our approach transforms each graph into a set of subgraphs and a coarsened graph based on a reduction ratio. As a result, each graph in the training set and test set gets reduced. From our results, we see that FIT-GNN outperforms all the baselines.

Table 14 and 15 present the ablation study on various coarsening algorithms for all the aforementioned tasks. From the results, we observe that **variation_neighborhoods** coarsening algorithm yields consistently better results compared to others.

Table 7: Results on Graph Classification with accuracy as metric (higher is better). We use the extra nodes method and **Gc-train-to-Gc-infer** as experimental setup. **algebraic_JC** coarsening algorithm is used.

Methods	Models	Graph per class	Dataset	
			AIDS	*PROTEINS*
DOSCOND	GCN	1	0.785	0.590
		10	0.666	0.647
		50	0.518	0.656
	GAT	1	0.608	0.652
		10	0.723	0.667
		50	0.729	0.657
KIDD	GCN	1	0.399	0.416
		10	0.236	0.659
		50	0.252	0.671
	GAT	1	0.441	0.416
		10	0.225	0.665
		50	0.218	0.671
	SAGE	1	0.653	0.416
		10	0.361	0.650
		50	0.283	0.673
	GIN	1	0.759	0.412
		10	0.637	0.655
		50	0.634	0.674

Methods	Models	Reduction Ratio (r)	Dataset	
			AIDS	*PROTEINS*
Full	GCN	1.0	0.788	0.710
	GAT	1.0	0.802	0.645
	SAGE	1.0	0.770	0.613
	GIN	1.0	0.800	0.774
FIT-GNN	GCN	0.1	0.810	0.783
		0.3	**0.844**	**0.826**
		0.5	0.836	0.696
		0.7	0.793	0.783
	GAT	0.1	0.784	0.652
		0.3	0.793	0.522
		0.5	0.810	0.739
		0.7	0.759	0.522
	SAGE	0.1	0.793	0.696
		0.3	0.828	0.696
		0.5	0.793	0.696
		0.7	0.819	**0.826**
	GIN	0.1	0.819	0.652
		0.3	0.828	0.783
		0.5	0.793	0.478
		0.7	0.819	0.739

6.2 Inference Time and Memory

As mentioned in Section 4.3, our inference time is less than the standard GNN if certain conditions are met. In Table 8a and 8b, we club all baseline models into one, since all **baselines are inferred on the whole graph**. We empirically show the reduction of time and space by our FIT-GNN model during inference. For recording the inference time, we use the Python **time** package to calculate the difference in time before and after the inference step. In Table 8a, we show the average time to predict for 1000 queries (Prediction for

Table 8: Inference time (sec) (Lower is better) comparison for Node-Level tasks and Graph-Level tasks. We show single-node prediction time using two different coarsening ratios for Node-Level tasks. Here, we used **Cluster Nodes**. We used **Gc-train-to-Gc-infer** experimental setup for the graph-level tasks.

(a) Node-Level Tasks

		FIT-GNN	
Dataset	Baselines	r = 0.1	r = 0.3
Chameleon	0.0027	0.0016	**0.0014**
Squirrel	0.0081	0.0017	**0.0014**
Crocodile	0.0070	0.0015	**0.0015**
Cora	0.0026	**0.0019**	0.0020
Citeseer	0.0031	**0.0018**	0.0019
Pubmed	0.0042	0.0019	**0.0018**
DBLP	0.0063	0.0020	**0.0018**
Physics Coauthor	0.0252	0.0020	**0.0017**
OGBN-Products	0.1762	0.0017	**0.0016**

(b) Graph-Level Tasks

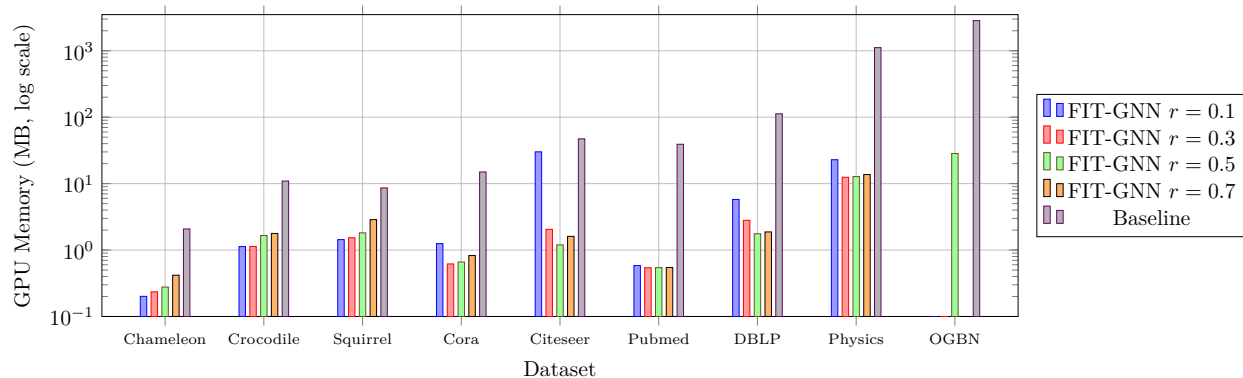|		FIT-GNN	
Dataset	Baselines	r = 0.3	r = 0.5
ZINC (subset)	**0.00184**	**0.00184**	0.00190
QM9	**0.00173**	0.00180	0.00191
AIDS	0.00163	**0.00155**	0.00163
PROTEINS	0.00165	**0.00160**	0.00163

Figure 4: GPU memory consumption in MegaBytes (MB) (log scale) for FIT-GNN (Cluster Node) at different reduction ratios r and Baseline, during inference. **variation_neighborhoods** coarsening algorithm is used.

Node v_i) in the Baseline and FIT-GNN models for node regression and classification tasks. The baseline model processes the entire graph, increasing inference time, especially for large graphs. In contrast, the FIT-GNN model only requires the relevant subgraph, resulting in faster predictions. For larger datasets like *OGBN-Products*, baseline inference is not feasible with our computational capacity. Therefore, to show a comparison, we take a subset of *OGBN-Products* with 165000 nodes and 4340428 edges with respect to which we see up to **100× speedup in inference time**. Section C elaborates more on the inference time for datasets with a larger number of nodes. Traditional methods fail to infer for very large datasets due to memory constraints. However, our approach enables inference on the whole graph. Figure 4 and Table 13 show the detailed comparison of memory consumption for different datasets for both Extra Nodes and Cluster Nodes methods, along with the baseline memory, which highlights that the FIT-GNN model uses up to **100× less memory** than the Baseline. Figure 6 shows the time taken to coarsen for different coarsening ratios for the *Cora* dataset. As the coarsening ratio increases, the time also increases, since the number of subgraphs increases.

Table 8b compares the inference time of graph classification and graph regression tasks. We predict for randomly selected 1000 graphs from the test split. The table shows how our method is comparable and sometimes faster than the Baseline. Also, we observe that the inference time increases with a higher coarsening ratio. Because with a higher coarsening ratio, the number of nodes in G' increases, resulting in more edges. Overall, the inference time and memory for all the tasks mentioned are drastically less than the baselines while maintaining the performance.

7 Conclusion

In this paper, we have focused on inference time and memory and presented a new way to utilize existing graph coarsening algorithms for GNNs. We have provided theoretical insight corresponding to the number of nodes in the graph for which the FIT-GNN model reduces the time and space complexity. Empirically, we have shown that our method is comparable to the uncoarsened Baseline while being orders of magnitude faster in terms of inference time and consuming a fraction of the memory. Future directions include extending the FIT-GNN methodology to directed, weighted, heterogeneous, and temporal graphs, alongside tackling data-intensive real-world challenges like weather forecasting. Theoretically, we aim to quantify the information loss for the Cluster Node method, investigate its connection to Extra Nodes, and explore novel strategies beyond both to further mitigate graph partitioning loss.

8 Acknowledgment

References

Jianfei Chen, Jun Zhu, and Le Song. Stochastic training of graph convolutional networks with variance reduction. In *International Conference on Machine Learning*, pp. 942–950. PMLR, 2018a.

Jie Chen, Tengfei Ma, and Cao Xiao. FastGCN: Fast learning with graph convolutional networks via importance sampling. In *International Conference on Learning Representations*, 2018b.

Wei-Lin Chiang, Xuanqing Liu, Si Si, Yang Li, Samy Bengio, and Cho-Jui Hsieh. Cluster-gcn: An efficient algorithm for training deep and large graph convolutional networks. In *Proceedings of the 25th ACM SIGKDD International Conference on Knowledge Discovery & Data Mining*, KDD '19, pp. 257–266. Association for Computing Machinery, 2019. ISBN 9781450362016.

Weilin Cong, Rana Forsati, Mahmut Kandemir, and Mehrdad Mahdavi. Minimal variance sampling with provable guarantees for fast training of graph neural networks. In *Proceedings of the 26th ACM SIGKDD International Conference on Knowledge Discovery & Data Mining*, KDD '20, pp. 1393–1403. Association for Computing Machinery, 2020. ISBN 9781450379984.

Charles Dickens, Edward Huang, Aishwarya Reganti, Jiong Zhu, Karthik Subbian, and Danai Koutra. Graph coarsening via convolution matching for scalable graph neural network training. In *Companion Proceedings of the ACM Web Conference 2024*, WWW '24, pp. 1502–1510, New York, NY, USA, 2024. Association for Computing Machinery. ISBN 9798400701726. doi: 10.1145/3589335.3651920. URL `https://doi.org/10.1145/3589335.3651920`.

Matthew Fahrbach, Gramoz Goranci, Richard Peng, Sushant Sachdeva, and Chi Wang. Faster graph embeddings via coarsening. In *international conference on machine learning*, pp. 2953–2963. PMLR, 2020.

C. Lee Giles, Kurt D. Bollacker, and Steve Lawrence. Citeseer: an automatic citation indexing system. In *Proceedings of the Third ACM Conference on Digital Libraries*, DL '98, pp. 89–98. Association for Computing Machinery, 1998. ISBN 0897919653.

Justin Gilmer, Samuel S Schoenholz, Patrick F Riley, Oriol Vinyals, and George E Dahl. Neural message passing for quantum chemistry. In *International conference on machine learning*, pp. 1263–1272. Pmlr, 2017.

Rafael Gómez-Bombarelli, Jennifer N Wei, David Duvenaud, José Miguel Hernández-Lobato, Benjamín Sánchez-Lengeling, Dennis Sheberla, Jorge Aguilera-Iparraguirre, Timothy D Hirzel, Ryan P Adams, and Alán Aspuru-Guzik. Automatic chemical design using a data-driven continuous representation of molecules. *ACS central science*, 4(2):268–276, 2018.

Mridul Gupta, Samyak Jain, Vansh Ramani, Hariprasad Kodamana, and Sayan Ranu. Bonsai: Gradient-free graph condensation for node classification. In *The Thirteenth International Conference on Learning Representations*, 2025.

Weihua Hu, Matthias Fey, Marinka Zitnik, Yuxiao Dong, Hongyu Ren, Bowen Liu, Michele Catasta, and Jure Leskovec. Open graph benchmark: datasets for machine learning on graphs. In *Proceedings of the 34th International Conference on Neural Information Processing Systems*, NIPS '20. Curran Associates Inc., 2020. ISBN 9781713829546.

Zengfeng Huang, Shengzhong Zhang, Chong Xi, Tang Liu, and Min Zhou. Scaling up graph neural networks via graph coarsening. In *Proceedings of the 27th ACM SIGKDD Conference on Knowledge Discovery & Data Mining*, KDD '21, pp. 675–684. Association for Computing Machinery, 2021. ISBN 9781450383325.

Wei Jin, Lingxiao Zhao, Shichang Zhang, Yozen Liu, Jiliang Tang, and Neil Shah. Graph condensation for graph neural networks. In *International Conference on Learning Representations*, 2021.

Wei Jin, Xianfeng Tang, Haoming Jiang, Zheng Li, Danqing Zhang, Jiliang Tang, and Bing Yin. Condensing graphs via one-step gradient matching. In *Proceedings of the 28th ACM SIGKDD Conference on Knowledge Discovery and Data Mining*, KDD '22, pp. 720–730. ACM, August 2022. doi: 10.1145/3534678.3539429. URL http://dx.doi.org/10.1145/3534678.3539429.

Antonin Joly and Nicolas Keriven. Graph coarsening with message-passing guarantees. *Advances in Neural Information Processing Systems*, 37:114902–114927, 2024.

Mohit Kataria, Sandeep Kumar, and Jayadeva. Ugc: Universal graph coarsening. In A. Globerson, L. Mackey, D. Belgrave, A. Fan, U. Paquet, J. Tomczak, and C. Zhang (eds.), *Advances in Neural Information Processing Systems*, volume 37, pp. 63057–63081. Curran Associates, Inc., 2024. URL https://proceedings.neurips.cc/paper_files/paper/2024/file/733209a1f12071a7ec979e8ffaeb1d99-Paper-Conference.pdf.

Thomas N. Kipf and Max Welling. Semi-Supervised Classification with Graph Convolutional Networks. In *ICLR*, 2017.

Manoj Kumar, Anurag Sharma, Shashwat Saxena, and Sandeep Kumar. Featured graph coarsening with similarity guarantees. In Andreas Krause, Emma Brunskill, Kyunghyun Cho, Barbara Engelhardt, Sivan Sabato, and Jonathan Scarlett (eds.), *Proceedings of the 40th International Conference on Machine Learning*, volume 202 of *Proceedings of Machine Learning Research*, pp. 17953–17975. PMLR, 23–29 Jul 2023.

Juncheng Liu, Bryan Hooi, Kenji Kawaguchi, Yiwei Wang, Chaosheng Dong, and Xiaokui Xiao. Scalable and effective implicit graph neural networks on large graphs. In *The Twelfth International Conference on Learning Representations*, 2024.

Andreas Loukas. Graph reduction with spectral and cut guarantees. *Journal of Machine Learning Research*, 20(116):1–42, 2019.

Yuankai Luo, Lei Shi, and Xiao-Ming Wu. Classic GNNs are strong baselines: Reassessing GNNs for node classification. In *The Thirty-eight Conference on Neural Information Processing Systems Datasets and Benchmarks Track*, 2024. URL https://openreview.net/forum?id=xkljKdGe4E.

Andrew Kachites McCallum, Kamal Nigam, Jason Rennie, and Kristie Seymore. Automating the construction of internet portals with machine learning. *Information Retrieval*, 3(2):127–163, Jul 2000. ISSN 1573-7659.

Christopher Morris, Nils M. Kriege, Franka Bause, Kristian Kersting, Petra Mutzel, and Marion Neumann. Tudataset: A collection of benchmark datasets for learning with graphs. In *ICML 2020 Workshop on Graph Representation Learning and Beyond (GRL+ 2020)*, 2020.

Benedek Rozemberczki, Carl Allen, and Rik Sarkar. Multi-scale attributed node embedding. *Journal of Complex Networks*, 9(2):cnab014, 2021.

Prithviraj Sen, Galileo Namata, Mustafa Bilgic, Lise Getoor, Brian Galligher, and Tina Eliassi-Rad. Collective classification in network data. *AI Magazine*, 29(3):93, Sep. 2008.

Oleksandr Shchur, Maximilian Mumme, Aleksandar Bojchevski, and Stephan Günnemann. Pitfalls of graph neural network evaluation. *Relational Representation Learning Workshop, NeurIPS 2018*, 2018.

Jie Tang, Jing Zhang, Limin Yao, Juanzi Li, Li Zhang, and Zhong Su. Arnetminer: extraction and mining of academic social networks. In *Proceedings of the 14th ACM SIGKDD International Conference on Knowledge Discovery and Data Mining*, KDD '08, pp. 990–998. Association for Computing Machinery, 2008. ISBN 9781605581934.

Petar Veličković, Guillem Cucurull, Arantxa Casanova, Adriana Romero, Pietro Liò, and Yoshua Bengio. Graph attention networks. In *International Conference on Learning Representations*, 2018.

Lin Wang, Wenqi Fan, Jiatong Li, Yao Ma, and Qing Li. Fast graph condensation with structure-based neural tangent kernel. In *Proceedings of the ACM Web Conference 2024*, pp. 4439–4448, 2024.

Zhenqin Wu, Bharath Ramsundar, Evan N Feinberg, Joseph Gomes, Caleb Geniesse, Aneesh S Pappu, Karl Leswing, and Vijay Pande. Moleculenet: a benchmark for molecular machine learning. *Chemical science*, 9(2):513–530, 2018.

Zhe Xu, Yuzhong Chen, Menghai Pan, Huiyuan Chen, Mahashweta Das, Hao Yang, and Hanghang Tong. Kernel ridge regression-based graph dataset distillation. In *Proceedings of the 29th ACM SIGKDD Conference on Knowledge Discovery and Data Mining*, KDD '23, pp. 2850–2861, New York, NY, USA, 2023. Association for Computing Machinery. ISBN 9798400701030. doi: 10.1145/3580305.3599398. URL https://doi.org/10.1145/3580305.3599398.

Zihui Xue, Yuedong Yang, and Radu Marculescu. Sugar: Efficient subgraph-level training via resource-aware graph partitioning. *IEEE Transactions on Computers*, 72(11):3167–3177, 2023.

Zhilin Yang, William W. Cohen, and Ruslan Salakhutdinov. Revisiting semi-supervised learning with graph embeddings. In *Proceedings of the 33rd International Conference on International Conference on Machine Learning - Volume 48*, ICML'16, pp. 40–48. JMLR.org, 2016.

Hanqing Zeng, Hongkuan Zhou, Ajitesh Srivastava, Rajgopal Kannan, and Viktor Prasanna. Graphsaint: Graph sampling based inductive learning method. In *International Conference on Learning Representations*, 2020.

Difan Zou, Ziniu Hu, Yewen Wang, Song Jiang, Yizhou Sun, and Quanquan Gu. Layer-dependent importance sampling for training deep and large graph convolutional networks. In *Proceedings of the 33rd International Conference on Neural Information Processing Systems*, pp. 11249–11259, 2019.

Appendix

A More on Extra Nodes and Cluster Nodes

A.1 Extra Nodes

Lemma 4.1. *Models with* 1 *layer of GNN cannot distinguish between G and $\mathcal{G}_s$ when **Extra Nodes** method is used.*

Proof. There are 2 sets of nodes in G_i as follows:

- The set S_1 of nodes with 1-hop neighbours in G_i.

- The set S_2 of nodes with not all 1-hop neighbors in G_i

Let $\mathcal{I}_i^1$ be the number of nodes whose information does not get passed on after 1 layer of GNN for G_i.

$$\mathcal{I}_i^1 = \left| \bigcup_{v \in S_2} \mathcal{N}_1(v) - V(G_i) \right|$$

$$\text{Now,} \left| \bigcup_{v \in S_1} \{u \in V : u \in \mathcal{N}_1(v) \wedge u \notin G_i\} \right| = 0$$

$$\text{Also,} \ \mathcal{E}_{G_i} = \bigcup_{v \in S_2} \{u \in V : u \in \mathcal{N}_1(v) \wedge u \notin G_i\}$$

$$\Rightarrow |\mathcal{E}_{G_i}| = \mathcal{I}_i^1$$

Hence, when **Extra Nodes** is used, 1 Layer GNN model cannot distinguish G and $\mathcal{G}_s$. $\qquad\square$

To understand the information loss when taking 2 Layers of GNN, we divide G_i into 3 sets of nodes.

- S_1: Nodes with 1-hop and 2-hop neighbours in G_i.

- S_2: Nodes with 1-hop neighbours in G_i but $\exists v$ in 2-hop neighbourhood that is not in G_i.

- S_3: Node where $\exists v$ in 1-hop and 2-hop neighbourhood that is not in G_i.

Let $\mathcal{I}_i^2$ be the number of nodes whose information doesn't get passed on after 2 layer of GNN for G_i.

$$\mathcal{I}_i^2 = \left| \bigcup_{v \in S_3} \mathcal{N}_2(v) - V(G_i) \right|$$

When we use **Extra Nodes**, the information loss can be written as follows:

$$\mathcal{I}_i^2 = \left| \bigcup_{v \in S_3} \mathcal{N}_2(v) - V(G_i) - \mathcal{E}_{G_i} \right|$$

The above entity will depend on the density of the subgraphs formed and the number of connections each subgraph shares with each other. An algorithm with an objective to reduce this entity for all subgraphs will lose the least amount of information when **Extra Nodes** method is used.

A.2 Cluster Nodes

Given a partition matrix P, the features of the coarsened node are $X' = P^\top X$. Given a normalized partition matrix, the features of a node $v_i' \in G'$ is the degree-weighted average of the features of nodes in C_i. This is one of the functions f used to create the features of the cluster node from C_i.

Previously, according to Lemma 4.1, there is no information loss when using the 1 layer of GNN and **Extra Nodes** method. It was also easy to quantify in terms of the number of nodes. However, it is different for **Cluster Nodes**. Let us discuss the issues first.

- Only a weighted version of node information is shared with the subgraph. Suppose $v_c, v_d \in G_i$ is connected to $v_a, v_b \in G_j$. Then the information contributed by these nodes is $\frac{d_a x_a + d_b x_b}{\sum_p d_p}$. Here d_p represents the degree of node v_p, and x_p represents the feature of node v_p.

- Other node information will also be shared which is $\frac{\sum_{p \neq v_a, v_b} d_p x_p}{\sum_p d_p}$. This will capture further dependencies.

The performance of **Cluster Node** will depend on some distance or similarity metric between x_c, x_d and $f(C_j)$.

B   More Algorithms

Algorithm 3 Training GNN (Train on G') (Huang et al., 2021)

Require: $G = (V, E, X)$; Labels Y; Node-Model M; Loss ℓ; Number of Layers L
1: Apply a coarsening algorithm on G, and output a normalized partition matrix P;
2: Construct Coarsened graph G' using P;
3: Construct feature matrix for G' by $X' = P^\top X$;
4: Construct labels for G' by $Y' = \arg\max(P^\top Y)$;
5: $O = M(L, A', D', X')$;   ▷ Algorithm 4
6: $Loss = \ell(O, Y')$;
7: Train M to minimize $Loss$;

Algorithm 4 Node-Model(L, A, D, X)

Require: Number of Layers L; A; D; $X^{(0)} = X$;
1: **for** $i = 1$ to L **do**
2: $\quad X^{(i)} = \sigma(\tilde{D}^{-\frac{1}{2}} \tilde{A} \tilde{D}^{-\frac{1}{2}} X^{(i-1)} \mathcal{W}^{(i-1)})$ ▷ Equation 1
3: **end for**
4: $Z = X^{(L)} \mathcal{W}^{(L)}$
5: **return** Z

Algorithm 5 Graph-Model-$G'(L, A', D', X')$

Require: Number of Layers L; A'; D'; $X^{(0)} = X'$
1: **for** $i = 1$ to L **do**
2: $\quad X^{(i)} = \sigma(\tilde{D}'^{-\frac{1}{2}} \tilde{A}' \tilde{D}'^{-\frac{1}{2}} X^{(i-1)} \mathcal{W}^{(i-1)})$ ▷ Equation 1
3: **end for**
4: $\bar{X} = \text{MaxPooling}(X^{(L)})$
5: $Z = \bar{X} \mathcal{W}^{(L)}$
6: **return** Z

C   More on Time and Space complexity

C.1   Comparison with Baseline

In Lemma 4.2, we provide the conditions that need to be satisfied for better space and time complexities.

For node-level tasks, to obtain lower FIT-GNN inference time complexity as compared to classical GNN, we want the following as per asymptotic analysis,

1. Baseline vs. Single-Node Inference:

$$\underbrace{n^2 d + n d^2}_{\text{Baseline Complexity}} \geq \underbrace{\max_i^k [\bar{n}_i^2 d + \bar{n}_i d^2]}_{\text{FIT-GNN Complexity}} \tag{4}$$

2. Baseline vs. Full-Graph Inference:

$$\underbrace{n^2 d + n d^2}_{\text{Baseline Complexity}} \geq \underbrace{\sum_{i=1}^{k} \left[(n_i + \phi_i)^2 d + (n_i + \phi_i) d^2 \right]}_{\text{FIT-GNN Complexity}} \tag{5}$$
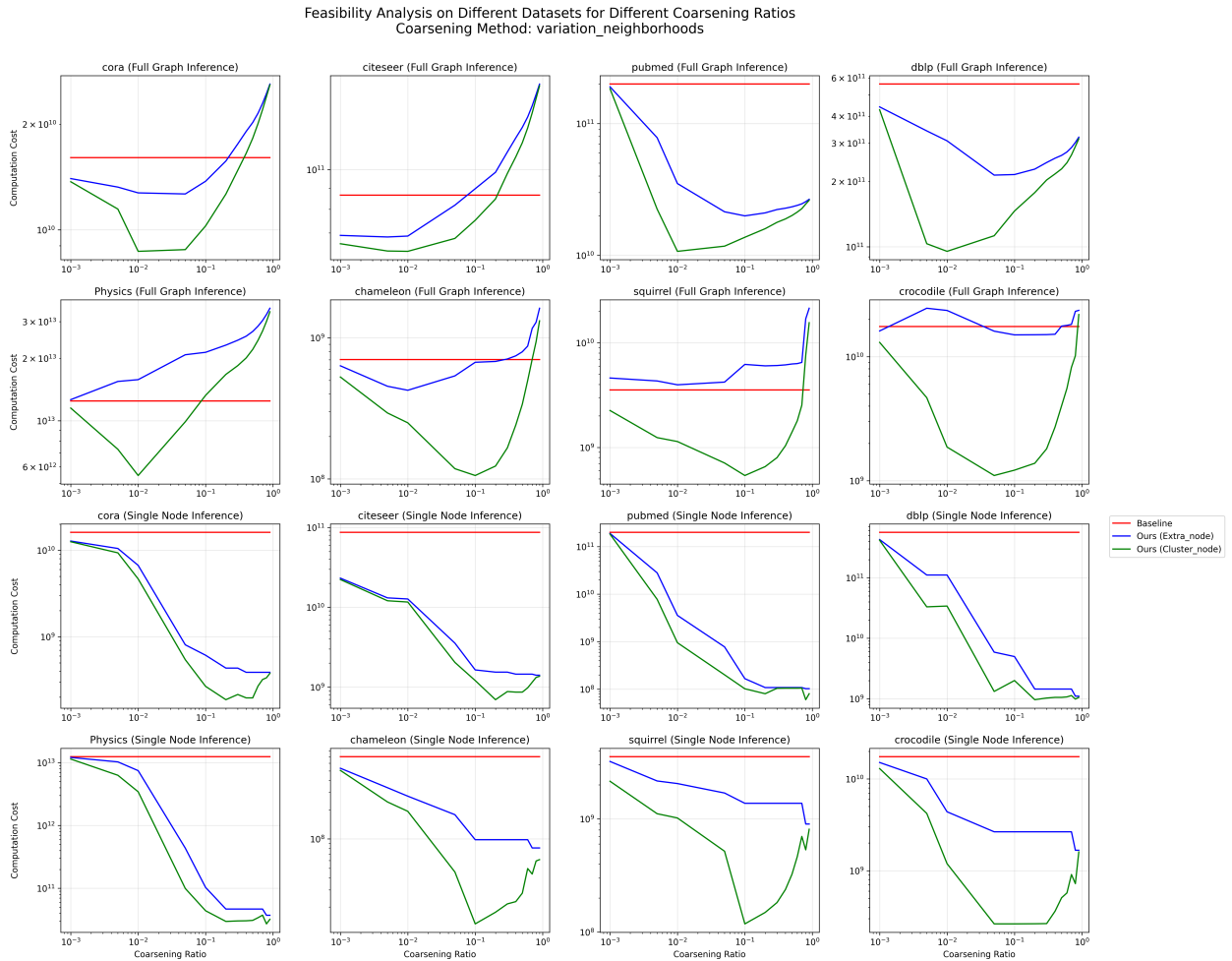
Figure 5: The figure shows the feasibility of our inference methods for different node-level datasets against coarsening ratios. Two important inference setups for each dataset: single-node inference with the computational cost $\mathcal{O}\left(\max_i (\bar{n}_i^2 d + \bar{n}_i d^2) + n\right)$, and full-graph inference with computational cost $\mathcal{O}\left(\sum_{i=1}^{k} (\bar{n}_i^2 d + \bar{n}_i d^2)\right)$, are compared against the baseline (classical GNN) computational cost of $\mathcal{O}\left(n^2 d + n d^2\right)$. The coarsening method used is variation_neighborhoods. Both axes are in logarithmic scale (base 10).

18

Figure 5 demonstrates the feasibility of our FIT-GNN method for different coarsening ratios with regards to full-graph inference time complexity. We empirically compute the LHS (baseline is classical GNN) and RHS of the Inequality 4 and 5 for various coarsening ratios and plot the results for multiple datasets. The coarsening algorithm used is variation_neighborhoods.

We make the following inferences:

1. There is a clear dataset-dependent computational-cost trade-off across different coarsening ratios. Moreover, the minimum inference time for our approach occurs at different coarsening ratios for different datasets.

2. Under single-node inference setup, FIT-GNN demonstrates increasingly superior inference time performance as compared to classical GNN with increasing coarsening ratio. This is because the individual subgraph sizes decrease with increasing coarsening ratio.

3. We observe lower inference time complexity of Cluster Node method as compared to Extra Node method under both inference setups. This is expected as $|C_{G_i}| \leq |\mathcal{E}_{G_i}|, \ \forall i \in \{1, 2, \ldots, k\}$.

C.2 Preprocessing Time Complexity

A comparative analysis of our preprocessing (coarsening) overhead against other state-of-the-art scaling methods has been conducted. As shown in the Table 9 below, our preprocessing time complexity is comparable to, and often faster than, existing SOTA methods. Thus, even when end-to-end latency is considered, FIT-GNN maintains its efficiency advantage.

Table 9: Asymptotic time complexities for different methods. N is the number of nodes in the original graph, M is the number of edges and C is the number of classes; rest of the symbols follow notation defined in Section 3 and 4. Blue and Red indicate CPU and GPU respectively - the hardware used for computation. Full Graph setup indicates testing on all the test nodes in a graph while Single Node setup represents testing for a single test node.

Method	Preprocessing	Training	Inference (Full Graph)	Inference (Single Node)	Model-Agnostic
SGGC	$M + N$	$k^2d + kd^2$	$N^2d + Nd^2$	$N^2d + Nd^2$	✓
GCOND	$C(N^2 + k^2)d$ $+C(N + k)d^2$	$k^2d + kd^2$	$N^2d + Nd^2$	$N^2d + Nd^2$	✗
BONSAI	$M + N$	$k^2d + kd^2$	$N^2d + Nd^2$	$N^2d + Nd^2$	✓
FIT-GNN	$M + N$	$kd^2 + k^2d$ $+ \sum_{i=1}^{k}[\bar{n}_i^2d + \bar{n}_id^2]$	$\sum_{i=1}^{k}[\bar{n}_i^2d + \bar{n}_id^2]$	$\max_i^k[\bar{n}_i^2d + \bar{n}_id^2]$	✓

We further extend our complexity analysis to the practical scenario, where a new test node v is introduced to the graph G. This setting is critical for real-world applications where graphs evolve dynamically. We compare three distinct inference strategies for this new node:

1. **Full Graph**: Construct G_{new} by adding v to the original full graph G and infer on G_{new} using the pre-trained network.

2. **2nd-hop Neighborhood**: Sample only the 2nd-hop neighborhood of v from G and infer using the pre-trained network (assuming a 2-layer architecture).

3. **FIT-GNN Subgraph**: Assign v to a relevant subgraph G_i (e.g., the one containing the majority of its 1st-hop neighborhood) and append the necessary Extra/Cluster nodes. Inference is then performed strictly within the modified subgraph G_i.

We present the time complexity comparison for these methods in the Table 10 below. The most significant advantage of the FIT-GNN approach is that inference complexity depends solely on the subgraph size $\bar{n}_i$ ($\bar{n}_i \ll n$). In contrast, the Full Graph approach remains tied to the global parameter n due to the necessity of accessing the full adjacency matrix.

Table 10: Time complexity of different inference strategies when a new node v is added to graph G

Inference Strategy	Preprocessing Complexity	Inference Complexity	Notes
Full Graph	$\mathcal{O}(1)$	$\mathcal{O}\left(n^2 d + n d^2\right)$	Computationally expensive; requires processing the entire graph for one new node.
2nd-hop Neighborhood	$\mathcal{O}\left(\|\mathcal{N}_1(v)\|\Delta^2\right)$	$\mathcal{O}\left(\|\mathcal{N}_2(v)\|^2 d + \|\mathcal{N}_2(v)\| d^2\right)$	$\|\mathcal{N}_j(v)\|$ is the number of nodes in j-hop neighborhood. Δ is the maximum degree in a graph.
FIT-GNN Subgraph	$\mathcal{O}(k)$	$\mathcal{O}\left(\bar{n}_i^2 d + \bar{n}_i d^2\right)$	Assuming v has maximum neighbors in G_i which has n_i many nodes.

D Dataset Description

(a) Summary of datasets used for Graph classification

Dataset	Number of Graphs	Average Nodes	Average Edges	Features	Classes
PROTEINS	1113	19	72	3	2
AIDS	2000	7	16	38	2

(b) Summary of datasets used for Graph regression

Dataset	Number of Graphs	Average Nodes	Average Edges	Features	Number of Targets
QM9	130831	8	18	11	19
ZINC (subset)	10000	11	25	1	1

(c) Summary of datasets used for Node classification

Dataset	Nodes	Edges	Features	Classes
Cora	2708	5278	1433	7
Citeseer	3327	4552	3703	6
Pubmed	19717	44324	500	3
DBLP	17716	52867	1639	4
Physics Coauthor	34493	247962	8415	5
OGBN-Products	2449029	61859140	100	47

(d) Summary of datasets used for Node regression

Dataset	Nodes	Edges	Features	Number of Targets
Chameleon	2277	31396	128	1
Squirrel	5201	198423	128	1
Crocodile	11631	170845	128	1

E Experiment Details (Parameters and Device Configuration)

For node classification and node regression tasks, we use Adam Optimizer with a learning rate of 0.01 and L_2 regularization with 0.0005 weight. We use Adam Optimizer with a learning rate of 0.0001 and L_2 regularization with 0.0005 weight for graph-level tasks. We set epochs to 20 and the number of layers of GCN to 2 for training. We set the hidden dimensions for each layer of GCN to 512.

The device configurations are Intel(R) Xeon(R) Gold 5120 CPU @ 2.20GHz, 256GB RAM, NVIDIA A100 40GB GPU. We use Pytorch Geometric to train our models.

F Results

Table 12 presents the results on the node classification task with all the coarsening ratios $\{0.1, 0.3, 0.5, 0.7\}$. We did not compare our experiments with methods such as Cluster-GCN(Chiang et al., 2019) because the method focuses on reducing training time by sampling subgraphs for several iterations. During the inference phase, however, it still performs inference on the entire graph. Consequently, its inference performance would be at most comparable to that of a standard GCN.

Figure 6 shows the time comparison for creating the subgraphs for *Cora* Dataset for different coarsening ratios. It is observed that the None method takes the least amount of time, which is intuitive since the subgraphs are not appended with additional nodes. For the Extra Node Method, the time increases since the subgraph size increases as new nodes are appended. For Cluster Node, we observe the maximum time taken since we are not only looking at the neighboring nodes that are lost due to partition, but also are

Table 12: Results for node classification tasks with accuracy as the metric (higher is better). We use the **Cluster Nodes** method to append additional nodes to subgraphs and **Gs-train-to-Gs-infer** as experimental setup. **variation_neighborhoods** coarsening algorithm is used.

Methods	Models	Reduction Ratio (r)	Dataset				
			Cora	*Citeseer*	*Pubmed*	*DBLP*	*Physics*
Full	GCN	1.0	0.821 ± 0.002	0.706 ± 0.002	0.768 ± 0.020	0.724 ± 0.002	0.933 ± 0.000
	GAT	1.0	0.809 ± 0.004	0.700 ± 0.003	0.740 ± 0.004	0.713 ± 0.004	0.909 ± 0.008
SGGC	GCN	0.1	0.752 ± 0.002	0.704 ± 0.003	0.730 ± 0.004	0.728 ± 0.019	0.892 ± 0.010
		0.3	0.808 ± 0.003	0.700 ± 0.001	0.773 ± 0.002	0.737 ± 0.011	0.928 ± 0.003
		0.5	0.808 ± 0.001	0.716 ± 0.002	$\mathbf{0.793 \pm 0.002}$	0.733 ± 0.008	0.931 ± 0.004
		0.7	0.805 ± 0.002	0.711 ± 0.003	0.786 ± 0.003	0.733 ± 0.014	0.931 ± 0.003
	GAT	0.1	0.630 ± 0.001	0.605 ± 0.025	0.689 ± 0.033	0.606 ± 0.017	0.854 ± 0.008
		0.3	0.686 ± 0.010	0.635 ± 0.021	0.773 ± 0.002	0.626 ± 0.028	0.870 ± 0.016
		0.5	0.641 ± 0.026	0.635 ± 0.024	0.683 ± 0.024	0.604 ± 0.047	0.842 ± 0.018
		0.7	0.643 ± 0.019	0.570 ± 0.041	0.733 ± 0.023	0.613 ± 0.018	0.851 ± 0.026
GCOND	GCN	0.1	0.789 ± 0.003	0.676 ± 0.020	0.785 ± 0.003	0.718 ± 0.007	0.884 ± 0.008
		0.3	0.806 ± 0.003	0.722 ± 0.001	0.779 ± 0.002	0.748 ± 0.001	0.876 ± 0.011
		0.5	0.808 ± 0.004	$\mathbf{0.730 \pm 0.007}$	0.773 ± 0.004	0.755 ± 0.002	0.804 ± 0.005
		0.7	0.793 ± 0.000	0.680 ± 0.012	0.775 ± 0.002	0.751 ± 0.000	0.914 ± 0.004
	GAT	0.1	0.657 ± 0.067	0.553 ± 0.116	0.511 ± 0.079	0.475 ± 0.057	OOM
		0.3	0.549 ± 0.080	0.628 ± 0.095	0.370 ± 0.079	0.481 ± 0.034	OOM
		0.5	0.712 ± 0.059	0.501 ± 0.085	0.409 ± 0.044	0.464 ± 0.030	OOM
		0.7	0.706 ± 0.062	0.453 ± 0.118	0.416 ± 0.036	0.462 ± 0.033	OOM
BONSAI	GCN	0.1	0.729 ± 0.008	0.576 ± 0.006	0.600 ± 0.098	0.699 ± 0.031	0.822 ± 0.014
		0.3	0.722 ± 0.011	0.585 ± 0.003	0.538 ± 0.103	0.683 ± 0.039	0.798 ± 0.007
		0.5	0.701 ± 0.012	0.666 ± 0.001	0.670 ± 0.084	0.702 ± 0.049	0.832 ± 0.016
		0.7	0.705 ± 0.009	0.582 ± 0.007	0.474 ± 0.020	0.694 ± 0.023	0.844 ± 0.015
	GAT	0.1	0.685 ± 0.004	0.589 ± 0.002	0.446 ± 0.014	0.642 ± 0.015	0.803 ± 0.005
		0.3	0.680 ± 0.014	0.566 ± 0.003	0.540 ± 0.096	0.665 ± 0.027	0.791 ± 0.010
		0.5	0.683 ± 0.006	0.579 ± 0.004	0.523 ± 0.133	0.681 ± 0.025	0.812 ± 0.016
		0.7	0.703 ± 0.010	0.594 ± 0.002	0.497 ± 0.028	0.705 ± 0.047	0.799 ± 0.010
FIT-GNN	GCN	0.1	0.790 ± 0.004	0.701 ± 0.001	0.757 ± 0.002	0.755 ± 0.001	0.909 ± 0.000
		0.3	0.800 ± 0.003	0.679 ± 0.003	0.754 ± 0.001	$\mathbf{0.786 \pm 0.001}$	$\mathbf{0.932 \pm 0.000}$
		0.5	$\mathbf{0.829 \pm 0.002}$	0.668 ± 0.003	0.761 ± 0.004	0.700 ± 0.001	0.926 ± 0.000
		0.7	0.813 ± 0.002	0.664 ± 0.001	0.756 ± 0.002	0.746 ± 0.001	0.925 ± 0.000
	GAT	0.1	0.773 ± 0.021	0.694 ± 0.003	0.737 ± 0.002	0.729 ± 0.010	0.887 ± 0.003
		0.3	0.761 ± 0.004	0.655 ± 0.005	0.754 ± 0.002	0.771 ± 0.002	0.885 ± 0.004
		0.5	0.792 ± 0.003	0.669 ± 0.004	0.760 ± 0.003	0.720 ± 0.002	0.885 ± 0.003
		0.7	0.797 ± 0.003	0.662 ± 0.003	0.759 ± 0.002	0.739 ± 0.002	0.903 ± 0.003

keeping a track of the cluster to which these neighboring nodes belong, corresponding to which, we add the cross-cluster edges.
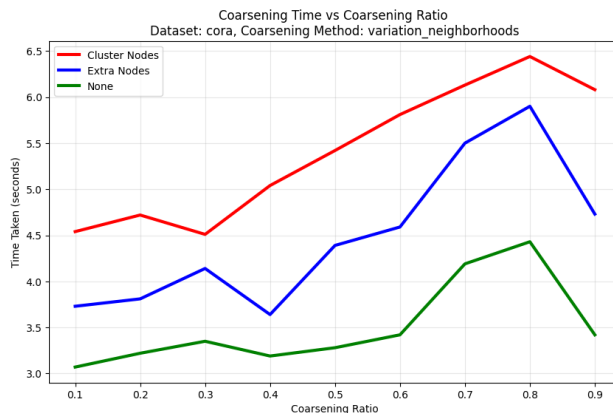

Figure 6: The plot shows how the coarsening time varies for the *Cora* dataset for different coarsening ratios using different methods of appending nodes to the subgraphs. **variation_neighborhoods** coarsening algorithm is used.

Table 13 shows the maximum GPU memory consumption during inference for different datasets with different coarsening ratios and methods of appending nodes. Note that this memory consumption is to store the graph and the weight matrix in the memory only.

Table 13: Summary of maximum GPU memory consumption during inference of datasets used for node-level tasks. All units are in MegaBytes (MB)

Dataset	Appending Nodes	FIT-GNN				Baseline
		r= 0.1	r= 0.3	r= 0.5	r= 0.7	
Chameleon	Cluster Node	0.201	0.235	0.277	0.418	2.078
	Extra Node	0.622	0.622	0.622	0.564	
Crocodile	Cluster Node	1.127	1.132	1.654	1.779	10.937
	Extra Node	4.586	4.586	4.586	4.586	
Squirrel	Cluster Node	1.436	1.532	1.815	2.869	8.614
	Extra Node	7.190	7.190	7.190	7.190	
Cora	Cluster Node	1.249	0.618	0.661	0.827	14.992
	Extra Node	1.906	1.103	0.970	0.970	
Citeseer	Cluster Node	30.097	2.048	1.195	1.607	47.170
	Extra Node	30.097	2.490	1.835	1.835	
Pubmed	Cluster Node	0.584	0.542	0.544	0.546	39.166
	Extra Node	0.778	0.562	0.562	0.562	
DBLP	Cluster Node	5.785	2.803	1.761	1.875	112.514
	Extra Node	28.271	6.008	2.308	2.207	
Physics Coauthor	Cluster Node	22.911	12.481	12.767	13.688	1115.079
	Extra Node	41.066	19.936	19.936	19.936	
OGBN-Products	Cluster Node	–	–	28.399	–	2840.706

To validate the use of "variation_neighborhoods" as a coarsening algorithm for all the results presented, we show an ablation study for different coarsening algorithms in Table 14 and 15.

Table 14: The table shows the FIT-GNN ablation study to compare various coarsening methods on *Cora* and *Chameleon* datasets, and the metrics for each dataset are accuracy (higher the better) and normalized MAE (lower the better), respectively.

	Cora		*Chameleon*	
Coarsening Method	**r = 0.1**	**r = 0.3**	**r = 0.1**	**r = 0.3**
variation_neighborhoods	0.790 ± 0.004	0.800 ± 0.003	0.496 ± 0.005	0.489 ± 0.003
algebraic_JC	0.827 ± 0.006	0.804 ± 0.003	0.544 ± 0.005	0.504 ± 0.003
kron	0.758 ± 0.004	0.800 ± 0.002	0.571 ± 0.004	0.580 ± 0.013
heavy_edge	0.736 ± 0.012	0.773 ± 0.006	0.572 ± 0.002	0.531 ± 0.002
variation_edges	0.484 ± 0.006	0.471 ± 0.012	0.513 ± 0.003	0.542 ± 0.005
variation_cliques	0.751 ± 0.012	0.801 ± 0.009	0.674 ± 0.009	0.679 ± 0.008

Table 15: The table shows the FIT-GNN ablation study to compare various coarsening methods on *PROTEINS* and *ZINC (subset)* datasets. The metric for the *PROTEINS* dataset is accuracy (higher is better), and for the *ZINC (subset)* is normalized MAE (lower is better)

	PROTEINS		ZINC (subset)	
Coarsening Method	**r = 0.3**	**r = 0.5**	**r = 0.3**	**r = 0.5**
variation_neighborhoods	0.652	0.739	0.573	0.620
algebraic_JC	0.826	0.739	0.823	0.810
kron	0.522	0.652	0.663	1.201
heavy_edge	0.565	0.609	2.114	1.227
variation_edges	0.652	0.565	1.548	1.883
variation_cliques	0.696	0.652	0.689	0.742

G   Detailed Ablation Study on Node Regression Performance

To understand the counterintuitive performance gains observed in node regression tasks when using FIT-GNN, we conducted a comprehensive ablation study. Specifically, we isolated the source of the performance gap to determine why restricting inference to localized subgraphs outperforms full-graph inference.

G.1   Impact of Inference Input vs. Training Regime

Our first objective was to determine whether the performance gain stemmed from the training methodology itself or the structure of the input data (subgraphs) during inference. We evaluated two distinct setups on the Crocodile dataset using a GCN convolutional layer:

- **Setup A:** Train on subgraphs $\rightarrow$ Infer on the full graph.

- **Setup B:** Train on the full graph $\rightarrow$ Infer on the full graph.

Table 16: Comparison of training and inference setups to isolate the source of performance gains.

Train Setup	Inference Setup	Mean Absolute Error (MAE)
Full Graph	Full Graph	0.852
Subgraphs	Full Graph	0.865
Subgraphs (FIT-GNN)	Subgraphs	**0.364**

As shown in Table 16, the performance of Setup A and Setup B is nearly identical, indicating that training on subgraphs alone does not account for the drastic MAE reduction. The substantial performance leap in FIT-GNN only occurs when subgraphs are used as the inference input, confirming that the local structural input drives the improvement.

G.2   Subgraph Optimization Landscape

We further hypothesized that partitioning the graph into subgraphs presents a simpler optimization landscape for the model. To quantify this, we compared the variation of labels locally (within individual subgraphs) versus globally across the entire graph. We computed the Label Standard Deviation for node regression datasets and Label Entropy for node classification datasets.

Table 17: Comparison of global label variation versus average local subgraph variation.

Dataset	Metric Used	Global Variation	Subgraph Variation (Avg)
Cora	Entropy	1.8311	0.1245
Citeseer	Entropy	1.7533	0.1572
Chameleon	Standard Deviation	2.1329	0.0689
Squirrel	Standard Deviation	1.7639	0.1284

The results in Table 17 demonstrate that the variation of labels within individual subgraphs is drastically lower than the global variation. By coarsening the graph, we create local contexts that are statistically more homogeneous, allowing the GNN to specialize more effectively and navigate a smoother optimization landscape during inference.

G.3   Structural Information Loss and Implicit Adversarial Pruning

Finally, we investigated the role of structural information loss. Using a coarsening ratio of $r = 0.5$, we empirically computed the fraction of the 2nd-hop neighborhood lost for each node.

(a) *Citeseer* (Classification)

(b) *Cora* (Classification)

(c) *Squirrel* (Regression)
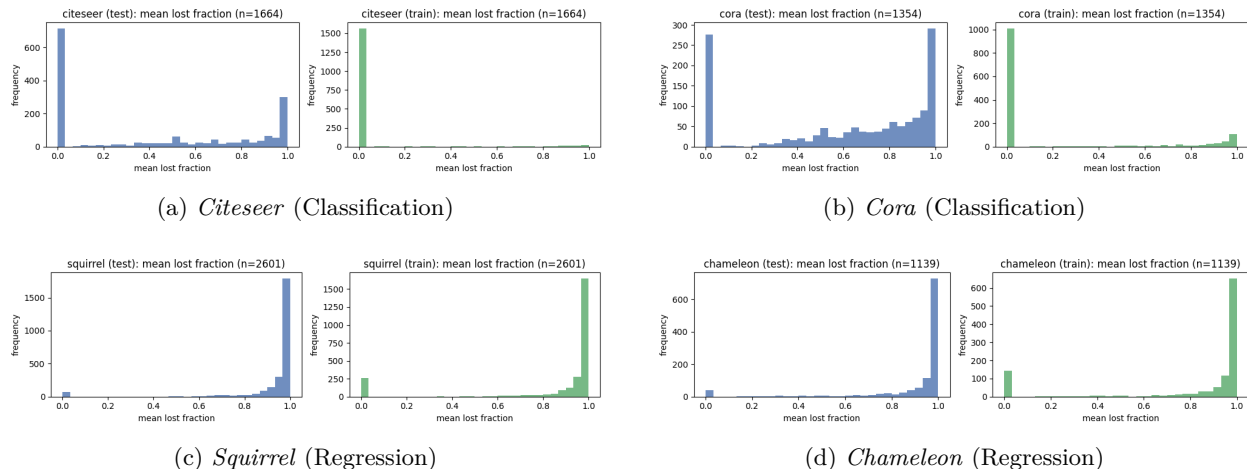
(d) *Chameleon* (Regression)

Figure 7: Histograms detailing the fraction of the 2nd-hop neighborhood lost for each node at a coarsening ratio of $r = 0.5$. A distinct difference in distribution is visible between classification (a, b) and regression (c, d) datasets.

Observations and Interpretation: The histograms in Figure 7 reveal a stark contrast between task types. In the node classification datasets (Cora, Citeseer), a significant number of nodes retain their 2nd-hop neighborhood entirely (lost fraction close to 0). Conversely, in the node regression datasets (Squirrel, Chameleon), the vast majority of nodes lose a highly significant portion of their 2nd-hop neighborhood (lost fraction close to 1).

Given the superior performance of FIT-GNN on these regression tasks, we interpret this structural loss as a form of **implicit adversarial pruning**. In specific heterophilic graphs, long-range information (such as 2nd-hop neighbors) acts as noise or an adversarial signal. The coarsening algorithms utilized by FIT-GNN implicitly filter out this distant noise. This pruning allows the model to fully exploit the low-variance, highly homogeneous local structures identified in Section G, thereby drastically reducing regression error.